

RF self-interference cancellation by using photonic technology [Invited]

Xiuyou Han (韩秀友)*, Xinxin Su (苏鑫鑫), Shuanglin Fu (付双林), Yiyi Gu (谷一英), Zhenlin Wu (武震林), Xiaozhou Li (李晓洲), and Mingshan Zhao (赵明山)

School of Optoelectronic Engineering and Instrumentation Science, Dalian University of Technology, Dalian 116024, China

*Corresponding author: xyhan@dlut.edu.cn

Received February 23, 2021 | Accepted April 7, 2021 | Posted Online April 27, 2021

Radio frequency (RF) self-interference is a key issue for the application of in-band full-duplex communication in beyond fifth generation and sixth generation communications. Compared with electronic technology, photonic technology has the advantages of wide bandwidth and high tuning precision, exhibiting great potential to realize high interference cancellation depth over broad band. In this paper, a comprehensive overview of photonic enabled RF self-interference cancellation (SIC) is presented. The operation principle of photonic RF SIC is introduced, and the advances in implementing photonic RF SIC according to the realization mechanism of phase reversal are summarized. For further realistic applications, the multipath RF SIC and the integrated photonic RF SIC are also surveyed. Finally, the challenges and opportunities of photonic RF SIC technology are discussed.

Keywords: in-band full-duplex; radio frequency self-interference cancellation; microwave photonics.

DOI: [10.3788/COL202119.073901](https://doi.org/10.3788/COL202119.073901)

1. Introduction

With the tremendous growth of modern wireless communications, crowded spectra and waste of spectrum resources, which limit the application of various wireless technologies, become the important issues, especially in beyond fifth generation (B5G) and sixth generation (6G) communications. Therefore, it is increasingly urgent to enhance spectrum utilization efficiency and to increase the wireless network capacity. Compared with the traditional frequency division duplex (FDD) and time division duplex (TDD), the in-band full-duplex (IBFD) technology transmitting and receiving signals simultaneously at the same frequency, as shown in Fig. 1, can double the spectrum utilization efficiency and data transmission rate and has great potential application in the new generation of mobile communications and satellite communications^[1-3]. However, in the process of IBFD communication, the transmitting antenna and the receiving antenna are generally on the same platform, as shown in Fig. 2; the high-power signal sent from the transmitting antenna will interfere the low-power signal of interest (SOI) that is received by the receiving antenna, or even submerge it completely, which is called radio frequency (RF) self-interference or co-site interference^[4]. This kind of interference is at the same frequency as the SOI, so it is impossible to filter it out by a notch filter or to select the SOI by a narrow band-pass filter. Therefore, RF self-interference is a key issue to be resolved for the application of IBFD technology.

RF self-interference cancellation (SIC) includes spatial cancellation, analog domain cancellation, and digital domain cancellation^[5]. Spatial cancellation is to use the physical isolation and optimized antenna arrangement for interference cancellation before the interference signal enters the receiver^[6]. The analog domain cancellation is implemented before the analog-to-digital conversion (ADC). The reference signal is drawn from the transmitter (Tx), and, through phase and amplitude being tuned, it cancels the interference signal when they are combined to the ADC channel^[7]. Digital domain cancellation takes the transmitted digital signal as a reference, and, after estimating the amplitude and phase factors of the residual interference signal and adaptively adjusting the coefficients of the finite impulse response filters, it cancels the interference signal^[8]. In order to realize the IBFD communications, the three RF SIC methods

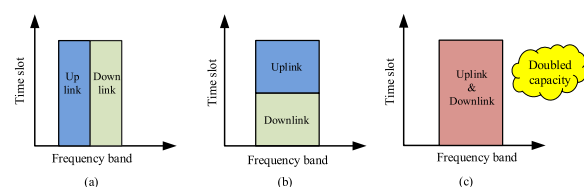


Fig. 1. Schematic of duplex technology for wireless communication. (a) Frequency division duplex, (b) time division duplex, and (c) in-band full duplex.

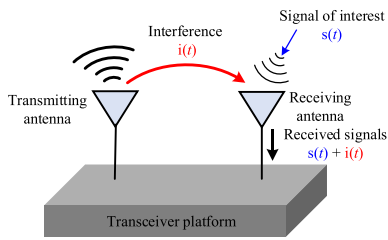


Fig. 2. Schematic of the RF self-interference during IBFD communication.

are usually utilized in combination to suppress the RF self-interference. Analog domain cancellation is an important stage to achieve RF SIC functionality^[9]. On the one hand, it suppresses RF self-interference to enough low-power levels to ensure that the ADC unit works within the dynamic range; on the other hand, it implements RF SIC in a wide bandwidth to meet the requirement of broadband IBFD communications. The electronic methods for analog domain RF SIC are limited by the bandwidth and the amplitude and phase control precision of RF devices, and it is difficult to obtain high SIC depth in a wide bandwidth.

Microwave photonics (MWP) brings together the worlds of RF engineering and optoelectronics focusing on not only military applications but also civil applications^[10–13]. MWP provides a considerable added value to traditional microwave and RF systems, as photonics allows the realization of key functionalities in these systems by virtue of the intrinsic advantages of ultrawide bandwidth and immunity to electromagnetic interference (EMI)^[14,15]. Photonic RF SIC technology leverages the advantage of high precision of time and amplitude control of microwave signals over broad band in the optical domain and exhibits great potential capability of suppressing RF self-interference for IBFD communications. It has been attracting more and more attention from not only academics but also the industry^[16].

This paper gives a review of photonic RF SIC technology for IBFD communications. The rest of this paper is organized as follows. In Section 2, the basic operation principle of photonic RF SIC is introduced, and the implementation of each functional unit in the photonic RF SIC system is briefly described. In Section 3, the advances of photonic RF SIC are classified and summarized according to realizing the out-of-phase relationship between the reference and interference paths. In Section 4, for orientating realistic applications, the multipath RF SIC by photonic methods is surveyed. In Section 5, the newly developed RF SIC by the photonic integration platform is presented. In the final section, a conclusion is drawn, and the perspective of development trends and issues to be solved for the application of photonic RF SIC is provided.

2. Operation Principle of Photonic RF SIC

The photonic RF SIC system for full-duplex communications is shown in Fig. 3. The high-power signal from the transmitting antenna will crosstalk into the receiving antenna and cause

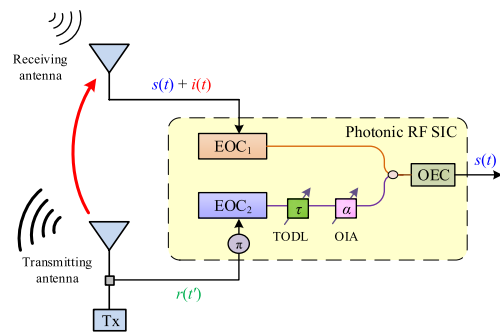


Fig. 3. Schematic diagram of photonic RF SIC for IBFD communication system.

interference to the low-power SOI. The operation principle of the photonic RF SIC is to establish a reference path in the optical domain and utilize the physical mechanism of interference cancellation to eliminate the RF self-interference. As shown in Fig. 3, the SOI $s(t)$ and the interference signal $i(t)$ received by the receiving antenna are converted to the optical domain by the electrical-to-optical converter (EOC_1), which is called the interference path. A reference signal $r(t)$ split from the Tx is also converted to the optical domain by EOC_2 , which is called the reference path. The optically carried RF signal in the reference path passes through the tunable optical delay line (TODL) and the optical intensity adjuster (OIA) and then enters the optical-to-electrical converter (OEC) together with the optically carried RF signal in the interference path. By adjusting the delay and amplitude of the optically carried RF reference signal via the TODL and OIA, respectively, the cancellation conditions between the reference and interference signals of equal amplitude, matching delay, and opposite phase can be realized. The interference signal is cancelled by the reference signal, and then the SOI is recovered.

The EOCs implement the converting of RF interference and reference signals into the optical domain. They can be the directly modulated lasers^[17,18], electro-absorption modulated lasers^[19–23], electro-absorption modulators^[24], electro-optic phase modulators^[25–27], polarization modulators (PolMs)^[28–30], Mach-Zehnder (MZ) electro-optic modulators (EOMs)^[31–33], or other MZ modified modulators^[34–37].

For time delay tuning in the optical domain, it can be realized by the DC motor driving optically tunable delay line^[18,25], the bit-switched optical delay line^[38], the cascaded waveguide-ring-based continuously tunable delay line^[39,40], the fiber-Bragg-grating-based delay line^[41,42], or the dispersive element through adjusting the wavelengths of the tunable lasers (TLs)^[29]. For amplitude adjusting in the optical domain, it can be actualized by the thermo-optic variable optical attenuator (VOA)^[38], the microelectromechanical-systems (MEMS)-based VOA^[25,42], or the semiconductor optical amplifier (SOA)^[43,44].

The OEC implements the converting of RF interference and reference signals from the optical domain to the electrical domain. It can be a common photodetector (PD)^[18,19,25–29,31–39,41–44], a multimode PD^[21,30] or a balanced PD (BPD)^[17,20,22–24,40,45].

3. Phase Reversal for Photonic RF Self-Interference Cancellation

Section 2 presents the operation principle of photonic RF SIC and summarizes the implementation methods of EOC, time delay tuning, amplitude tuning, and OEC. In order to realize the RF SIC, besides the conditions of equal amplitude and matching delay between the reference signal and the interference signal, the out-of-phase relationship should also be satisfied. The phase reversal can be achieved in the electrical domain or the optical domain. This section gives the research progress of photonic RF SIC according to the implementation physical mechanism of phase reversal.

3.1. Phase reversal in electrical domain

The electronic method for phase reversal brings a phase shift of π to the reference signal in the electrical domain before EOC or after OEC. Balun is a common electronic device, as shown in Fig. 4(a), with the functionality of splitting the RF signal into two paths with equal amplitude but opposite phase. The reference signal is generally tapped for the Tx, as shown in Fig. 3, and therefore Balun can be utilized as the splitter to implement a phase shift of π before EOC^[19,21,44]. As an electronic device, Balun may limit the operational frequency range of the photonic RF SIC systems.

The phase reversal can also be implemented after OEC usually by a BPD. As shown in Fig. 4(b), the BPD has dual photodiodes to receive optically carried RF signals and performs the optical-to-electrical conversion with differential outputs. Equivalently, the two output electrical signals have a phase difference of π . The BPD can be applied with a combination of two separate directly modulated lasers^[17], electro-absorption modulated lasers^[22–45], and electro-absorption modulators^[24,40] in the photonic RF SIC systems. By using the balanced detection of BPD, the common-mode noise of the microwave photonic links (MPLs) can be suppressed^[46,47], which is helpful for recovering the SOI.

3.2. Phase reversal in optical domain

When phase reversal is implemented in the optical domain, the operating frequency range would not be limited by the electronic devices. The dual MZ modulators (MZMs)-based photonic RF SIC system was firstly, to the best of our knowledge, proposed to suppress the RF self-interference^[31]. As shown in Fig. 5, the transmission curve of the MZM is similar to the cosine square

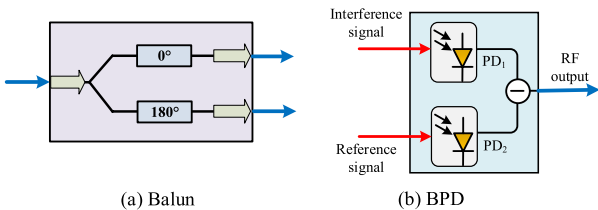


Fig. 4. Structure of optoelectronic devices to realize phase reversal.

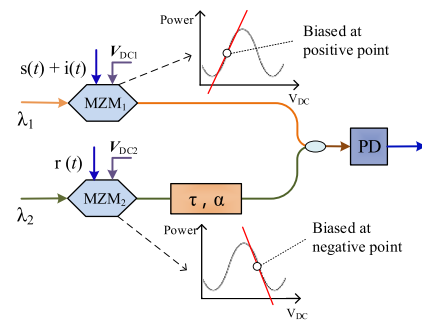


Fig. 5. Photonic RF SIC system with dual MZMs biased at reverse orthogonal points^[31].

function. By controlling the DC voltage, MZM1 in the interference path and MZM2 in the reference path are biased at the orthogonal points of the positive slope and the negative slope, respectively. Upon the EOC, the interference signal and the reference signal undergo the phase shift with the reversal relationship.

Since then, several MZ-based modulator structures for phase reversal in the optical domain have been put forward. The dual-drive MZM (DD-MZM), as shown in Fig. 6(a), with the interference signal input to one RF port and the reference signal into the other RF port, is biased at the minimum transmission point to obtain the phase reversal^[34]. However, the destructive interference between the optical carriers in the upper and lower arms degrades the gain of the photonic RF SIC system for recovering the SOI. To overcome this shortcoming, a dual-parallel MZM (DP-MZM), as shown in Fig. 6(b), is proposed to realize the phase reversal and amplitude tuning simultaneously by the DC controlled phase shifter (PS) in the lower arm of the

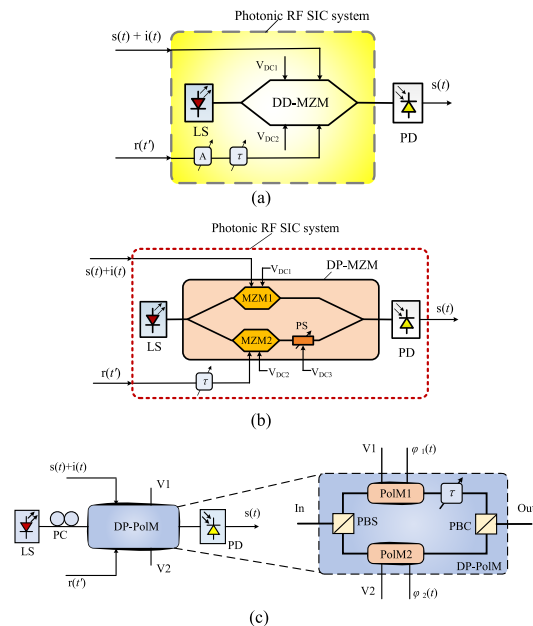


Fig. 6. Photonic RF SIC systems based on MZM-like structures for phase reversal: (a) DD-MZM^[34], (b) DP-MZM^[35], and (c) DP-PolM^[28].

DP-MZM^[35]. In Ref. [28], the dual-parallel PolM (DP-PolM), as shown in Fig. 6(c), composed of a polarization beam splitter, two PolMs, and a polarization beam combiner, is utilized as the equivalent dual MZMs, and the reversal phase is obtained by DC voltage control. In these MZ-based modulator structures, the bias voltage should be controlled accurately in order to maintain the exact out-of-phase condition, which may increase the complexity and cost of the photonic RF SIC systems.

The photonic RF SIC scheme based on phase modulation (PM) and optical sideband filtering without the need of DC bias voltage control is proposed in Ref. [25]. As shown in Fig. 7, the left and right sidebands of the RF phase-modulated signal have the inherent out-of-phase relationship^[48]. After optical sideband filtering, the phase reversal between the reference signal of left single sideband and the interference signal of the right sideband is achieved. With no need of DC bias voltage control, the photonic RF SIC structure is simplified greatly and has a good stability. Furthermore, it has the potential capability of operating over an ultrawide frequency band because the phase reversal, delay, and amplitude tuning are all completed in the optical domain^[26]. Certainly, the optical filter with steep spectral edges and high extinction ratio, namely the box-like spectrum, should be developed in order to explore the low-frequency applications.

The phase reversal can also be realized by other physical mechanisms, such as the slow and fast light effect in SOAs. In an SOA, the slow and fast light effect generates a tunable delay or phase shift by changing the propagating group velocity in the semiconductor using carrier dynamics^[49]. The SOA-based photonic RF SIC system is illustrated in Fig. 8^[43], where the SOA controls the phase shift and amplitude of the optically carried

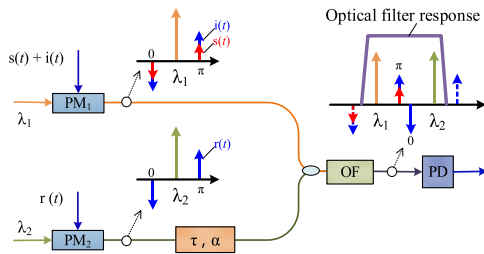


Fig. 7. Photonic RF SIC system based on phase modulation and optical sideband filtering^[25].

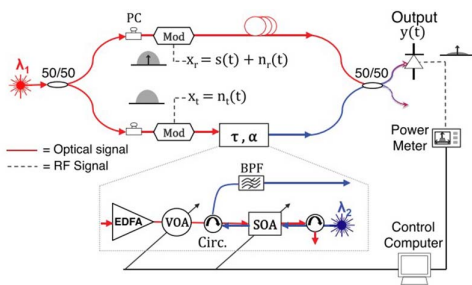
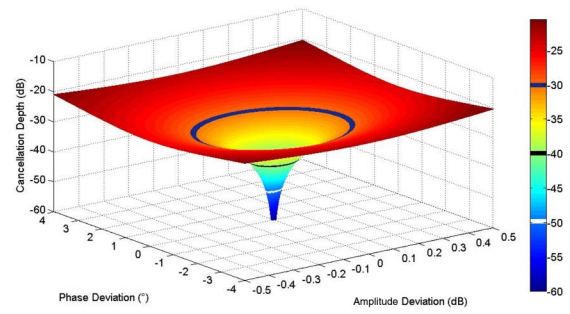


Fig. 8. Photonic RF SIC system based on slow and fast light effect in SOA^[43].

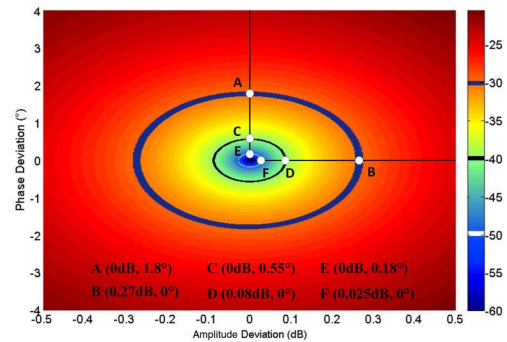
RF reference signal through adjusting the bias current and the input optical pump power via a VOA. The cross-gain modulation (XGM) is also utilized to transfer the reference signal to another wavelength carrier (λ_2), avoiding the coherent optical beat noise when combined with the interference signal carried by the optical carrier λ_1 . The advantages of the SOA-based photonic RF SIC scheme are the low latency of nanoseconds dictated by the semiconductor carrier lifetime and the potential high integration for fabricating the whole photonic RF SIC system on an integrated platform. The issue that should be considered is the trade-off between the microwave operation bandwidth and the induced magnitude of time delay^[50].

3.3. Photonic RF SIC performance

According to the cancellation principle, perfect cancellation can be obtained with the matching time delay, equal amplitude, and phase reversal between the reference signal and the interference signal. However, in the real application system, the three conditions may not be realized completely due to the environment vibration or the adjustment accuracy of TODL and OIA. The time delay mismatch induces the phase deviation eventually. The impact of the phase deviation and amplitude deviation on the cancellation depth is simulated based on the interference cancellation theory, and the results are illustrated in Fig. 9. Figure 9(a) shows the cancellation depth varying with the phase deviation $[-4^\circ, 4^\circ]$ and the amplitude deviation $[-0.5 \text{ dB}, 0.5 \text{ dB}]$ between the reference signal and the interference signal.



(a)



(b)

Fig. 9. Impact of amplitude deviation and phase deviation on the cancellation depth: (a) three-dimensional view and (b) top view.

Figure 9(b) shows the top view of Fig. 9(a), where three typical cancellation depths of 30 dB, 40 dB, and 50 dB are marked with circles. It can be seen that to achieve the cancellation depth of 30 dB, the allowable maximum phase deviation is 1.8° and the maximum amplitude deviation is 0.27 dB. The cancellation depth of 40 dB corresponds to the allowable maximum phase deviation of 0.55° and amplitude deviation of 0.08 dB. Similarly, achieving a 50 dB cancellation depth requires a maximum phase deviation of 0.18° and an amplitude deviation of 0.025 dB. To achieve a higher cancellation depth, higher adjustment accuracy of TODL and OIA is required with phase reversal over a broad bandwidth.

The representative experimental results of the above-mentioned photonic RF SIC schemes are summarized in Table 1, including the center frequency, bandwidth, and cancellation depth. It can be seen from Table 1 that the photonic RF SIC schemes can operate over a wide bandwidth with high cancellation depth, illustrating the outstanding performance compared with the electrical analog SIC systems^[51,52]. Certainly, there are still many different characteristics of the established photonic RF SIC systems. These mainly stem from the frequency response mismatches between the reference MPL and the interference MPL. One reason is that not exactly same optoelectronic components are utilized in both MPLs. The other reason is that the remaining RF components in the system have non-flat frequency responses, for example, the RF splitters. Therefore, to improve the performance of practical photonic RF SIC systems, the MPLs with well-matched frequency response should be fulfilled.

Table 1. Photonic RF Self-Interference Cancellation Results by Different Phase Reversal Methods.

Phase Reversal Methods	Center Frequency	Bandwidth	Cancellation Depth (dB)	Refs.
Balun	900 MHz	220 MHz	45	[19]
Balun	2.39 GHz	20 MHz	30	[21]
BPD	2.4 GHz	40 MHz	30	[24]
BPD	2.4 GHz	400 MHz	33	[17]
MZMs	3.0 GHz	100 MHz	30	[31]
MZMs	2.4 GHz	100 MHz	32.6	[32]
DP-PoIM	5.5 GHz	10 GHz	25	[28]
DD-MZM	2.4 GHz	300 MHz	32	[34]
DP-MZM	2.4 GHz	100 MHz	44	[36]
DP-MZM	4.5 GHz	200 MHz	42	[37]
PMs+filter	10 GHz	100 MHz	25.5	[26]
SOA	915 MHz	60 MHz	38	[43]
SOA	500 MHz	40 MHz	50	[44]

4. Multipath RF Self-interference Cancellation

In the realistic scenario of IBFD communications, RF self-interference is a combined result of direct path coupling from the Tx to the receiver as well as multiple transmission paths due to reflection, scattering, and diffraction from various terrain features. This is called multipath RF self-interference. Therefore, in order to realize IBFD communication, it is essential to complete multipath RF SIC. The following presents some representative photonic multipath RF SIC solutions.

4.1. Multipath RF SIC by SM-MM combiner

In Ref. [38], the photonic multipath RF SIC scheme is proposed by generating multiple reference signals through optical branching and using single-mode to multi-mode (SM-MM) couplers for combining. As shown in Fig. 10, the reference signal from the Tx is modulated onto the optical carrier via an MZM and then divided into multiple paths by the optical coupler. The optically carried RF reference signals in each path undergo different delay and amplitude adjustments and then combine with the interference signal via the SM-MM coupler into a multi-mode PD for optical-to-electrical conversion. The SM-MM coupler maps the optically carried RF signal in each single-mode fiber to distinguish the orthogonal spatial mode of the multi-mode fiber^[53], avoiding the coherent optical beat noise when the same frequency carriers are combined. A set of thermo-optic optical attenuators and tunable delay lines provide the amplitude and time adjustment for obtaining the matching cancellation conditions.

The interference cancellation up to the third multipath was demonstrated experimentally. The maximum cancellation depths of 40 dB over 200 MHz and 50 dB over 10 MHz were achieved around the 2.4 GHz range. Since only a single laser source is required, the photonic multipath RF SIC system is compact. The scalability of this scheme is determined by the number of orthogonal spatial modes that can be multiplexed by the SM-MM combiner. It relies on a coupling lens system and grows more complex with additional inputs^[54].

4.2. Multipath RF SIC by dispersion element

In Ref. [29], the photonic multipath RF SIC scheme using the dispersion element is proposed. As shown in Fig. 11, the

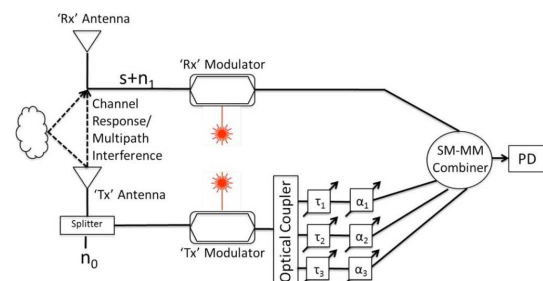


Fig. 10. Schematic of photonic multipath RF SIC system by SM-MM combiner^[38].

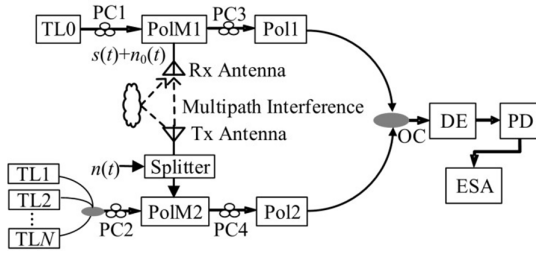


Fig. 11. Schematic of the photonic RF SIC system by using dispersion element^[29].

PolMs and the polarization controllers (PCs) are used to form the equivalent MZMs, which are biased at the quadrature bias point of positive and negative slopes, respectively. The reference signal from the Tx is modulated on the optical carriers from the TLs, which have different wavelengths, to form multipath reference signals. By utilizing the dispersion mechanism of the dispersion element, the delay in each reference path can be adjusted by changing the wavelength of the optical carrier from TL_i. In addition, the amplitude can be adjusted by tuning the output power of TL_i. A proof-of-concept experiment at the two-path interference case was performed. The cancellation depth of 44 dB with a bandwidth of 50 MHz was measured. With no need of the VOA and TODL, the system may be integrated easily with a compact volume. The PCs are utilized to conduct the equivalent MZM and to overcome the dispersion-induced RF power fading in the dispersive element^[55]. The stability of polarization states should be considered in the realistic applications.

4.3. Multipath RF SIC by PM and WDM

By virtue of no DC bias control requirement for PM, the photonic RF SIC scheme by wavelength division multiplexing (WDM) is proposed in Ref. [56]. As illustrated in Fig. 12, the tapped reference RF signals are phase modulated onto the optical carriers with different wavelengths, respectively, to construct multiple reference paths. The reference signals are also combined with the interference signal in the optical processor, which utilizes the diffraction grating and solid-state liquid crystal on silicon (LCoS) to implement the WDM functionality. Amplitude tuning and sideband filtering are completed simultaneously by the optical processor. The demonstration system with two-interference-path cancellation was constructed. The interference cancellation depths of 26 dB and 28 dB were obtained with the bandwidth of 100 MHz at the center frequencies of 6 GHz and 10 GHz, respectively. For a larger bandwidth, the cancellation depths of 25 dB over 240 MHz bandwidth and 15 dB over 4 GHz were obtained. By leveraging the advanced fiber optics communication technology^[57] and the powerful signal processing capability of LCoS^[58], the PM- and WDM-based photonic RF SIC scheme can deal with multipath RF self-interference with good scalability.

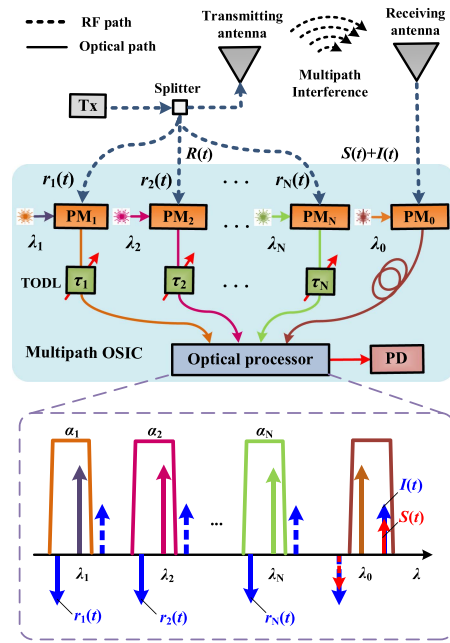


Fig. 12. Schematic of the photonic multipath RF SIC system by PM and WDM^[56].

4.4. Multipath RF SIC by FBG-based delay line

In Ref. [41], the photonic multipath RF SIC scheme using a fiber Bragg grating (FBG)-based delay line is proposed. As shown in Fig. 13, a 90° hybrid coupler is used to divide the input RF signal into an I component (upper part) and a Q component (lower part), and each component is modulated on the optical carrier from the TL via the MZM with differential output for phase inversion. FBGs with different reflection center wavelengths are cascaded in a fiber. A certain length fiber is inserted between every pair of FBGs to produce the delay time. When the wavelength of the TL is tuned to the corresponding reflection

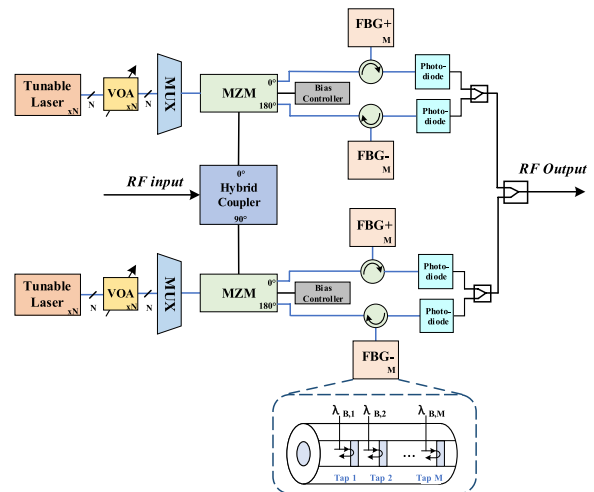


Fig. 13. Schematic of the photonic multipath RF SIC system by FBG-based delay lines^[41].

Table 2. Multipath Self-Interference Cancellation Schemes and Results.

Multipath Implementation	Center Frequency/GHz	Bandwidth/MHz	Cancellation Depth/dB	Refs.
SM-MM combiner	2.4	200	40	[38]
Dispersion element	3	50	44	[29]
PM and WDM	10	100	28	[56]
FBG-based delay line	0.5-5.5	500	25	[41]

wavelength of the FBG, the tap with a delay time is constructed, and the amplitude is adjusted by the VOA after the TL.

A 20 tap prototype with tunable time delay taps was measured with cancellations of 25 dB over 500 MHz bandwidth and 20 dB over 1 GHz and was tunable between 0.5 and 5.5 GHz. This scheme utilizes FBGs as the delay taps, which are fabricated in one optical fiber by mature ultraviolet writing technology and have the advantage of implementing high tap counts with low-loss delays and large delay spreads. Up to now, the delay adjustment of this scheme is discrete, and continuous delay tuning is desired^[42].

In order to show the performance of each multipath cancellation scheme more clearly, a summary is given in Table 2, which includes the key components for constructing multipath, center frequency, bandwidth, and interference cancellation results.

5. Photonic Integrated SIC Chip

In order to meet the application requirement of IBFD communications, especially for the mobile terminals in wireless communications^[59] and the new generation of satellite payloads^[60], the size, weight, and power (SWaP) must be taken into account for the photonic RF SIC. It is desirable to integrate the discrete optoelectronic devices onto a compact platform. Integrated MWP provides a potential way to fulfill the mission^[61]. This section gives the recent work of integrated photonic RF SIC chips on the indium phosphide (InP) platform and silicon platform.

5.1. Integrated photonic RF SIC chip on InP platform

InP is an active photonic material with the advantages of high integration and small size^[62,63]. In Ref. [64], a photonic integrated RF SIC chip based on the InP platform was demonstrated. As shown in Fig. 14, the distributed feedback (DFB) lasers with direction modulation, SOAs, and BPD are fabricated on the InP platform. The amplitude adjustment is generated by using optical absorption and stimulated emission in SOAs. The phase

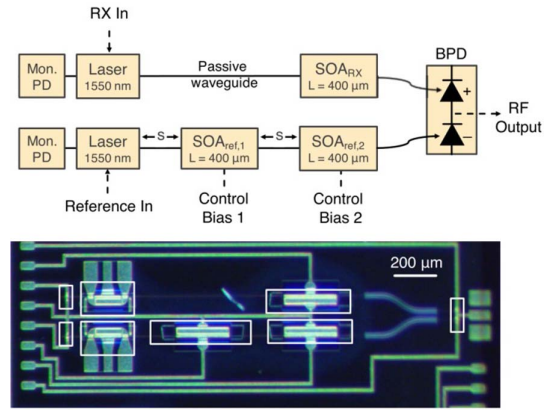


Fig. 14. Block diagram (top) and microscope image (bottom) of the integrated photonic RF SIC chip on InP platform^[64].

control is created by utilizing dispersion in the pair of SOAs driven into saturation.

The fabricated integrated photonic RF SIC chip was measured to operate from 400 MHz to 6 GHz and was able to cancel at least 30 dB of in-band interference with a bandwidth of 25 MHz across existing frequency division duplexed long term evolution (LTE) and wireless fidelity (WiFi) bands. The characterization of the integrated photonic RF SIC chip including RF gain, noise figure, linearity, and dynamic range was performed comprehensively as a function of RF frequency, laser bias, and SOA bias^[65]. It has only RF inputs and outputs and can potentially be integrated into RF circuit boards, greatly simplifying the installation of the canceller in RF front ends. Currently, the phase control approaches based on dispersion in SOAs inherently link together amplitude and phase via the Kramers–Krönig relations^[49,66]. The independent amplitude and phase control methods would be desirable, for example, for switching delays^[67].

5.2. Integrated photonic RF SIC chip on silicon platform

Silicon photonics utilizes high-index contrast materials for photonic integrated circuit manufacturing with the advantages of dense and large-scale integration of complex photonic functions, the compatibility with the current mature complementary metal-oxide semiconductor (CMOS) technology, and the potential of seamless integration with electronics^[68-70]. Our group recently has been carrying out the research on an integrated photonic RF SIC chip on the silicon platform^[39,71]. Figures 15(a) and 15(b) present, respectively, the schematic diagram and microscope image of the integrated photonic RF SIC chip fabricated by silicon photonics technology. As shown in Fig. 15(a), the PMs, TODL, IOA, optical filter, and PD are integrated on one chip. The continuous delay tuning is realized by the cascaded waveguide rings, the amplitude adjustment is obtained by the M interference (MZI)-based IOA, and the optical filter for sideband filtering is composed of a triple-ring assisted MZI structure. By optimizing the structure parameters of every unit in the photonic integrated RF SIC system, the chip was prepared on a silicon platform with the size of

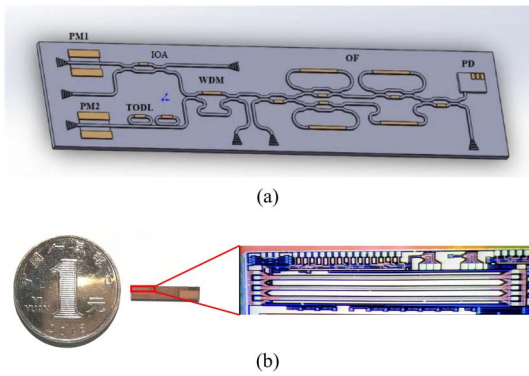


Fig. 15. (a) Schematic diagram and (b) microscope image of the integrated photonic RF SIC chip on silicon platform^[71].

1.2 mm × 5 mm, as shown in Fig. 15(b). The performance test and characterization are being conducted, and the results will be published in the future. Currently, the light sources are not integrated on the chip. With rapid development of heterogeneous integration of III-V materials onto the silicon photonic platform to overcome the challenge in producing light sources^[72], a full system-level integration of photonic RF SIC functionality on a single chip will come true.

6. Conclusion and Outlook

This paper reviewed the recent research on photonic RF SIC for IBFD communications. By introducing the operation principle of the photonic RF SIC, the development advances are summarized according to the realization mechanism of phase reversal in the electrical domain and optical domain. Aiming at the cancellation of multipath interference, the photonic RF SIC schemes by using the SM-MM combiner, dispersion element, PM and WDM, and FBG-based delay line are surveyed, and their pros and cons are analyzed. Finally, two types of integrated photonic SIC chips on the InP platform and silicon platform are presented.

The reported results demonstrate the advantages of photonic RF SIC technology, such as wide bandwidth, high cancellation depth, and operation over broad frequency band, showing the potential capacity to propel the IBFD communication application in B5G and 6G networks. Certainly, there are still some challenges for the photonic RF SIC technology going out of the laboratory and entering industrial applications that we should take a lot of effort to pursue, and also some new opportunities we could explore. The suggestions are listed as follows.

- (1) Demonstration of actual IBFD communications. The early work mainly focused on obtaining high cancellation depth and wide bandwidth of the photonic RF SIC system with the interference signal from the signal generator on the lab table. Few experiments were measured with transmitting and receiving antennas^[21,22,45,73]. Little attention was paid to the power ratio between the interference signal and the SOI^[20,56], which could determine the

feasibility of the photonic RF SIC system in actual IBFD communications. In addition, the systematic design and test of combining spatial cancellation, photonic-based analog cancellation, and digital cancellation should be proceeded for IBFD communications^[5,74].

- (2) Adaptive feedback control algorithm for photonic RF SIC. In realistic IBFD communications, the RF self-interference signals vary randomly, which entails the reference signals to change in time and adapt in order to suppress the interference effectively. Up to now, most of the photonic RF SIC systems achieve the best state of interference cancellation at static cases through manual adjustment of amplitude, delay, and phase. Therefore, the adaptive feedback control algorithm for the photonic RF SIC system should be incorporated^[64,73,75–77]. Fortunately, it can be learned from the algorithm of electrical RF SIC schemes.
- (3) Emerging with the new generation of broadband wireless networks. With the extensive deployment of the 5G network and the rapid development of the 6G network, photonic RF SIC technology can combine with microwave photonic signal processing schemes to enhance the capacity of the new generation broadband wireless network, such as the radio-over-fiber system to link optical network units^[73,78–80] and photonic RF front ends with frequency conversion^[81–86].

Acknowledgement

This work was supported in part by the National Key R&D Program of China (No. 2019YFB2203202), National Natural Science Foundation of China (Nos. 62075026 and 61875028), National Research Foundation of China (No. 61404130403), Program for Innovative Talents in Universities of Liaoning Province (No. LR2019017), Dalian Science and Technology Innovation Foundation (No. 2018J11CY006), and Fundamental Research Funds for the Central Universities (Nos. DUT18ZD106, DUT18GF102, and DUT18LAB20).

References

1. A. Sabharwal, P. Schniter, D. Guo, D. W. Bliss, S. Rangarajan, and R. Wichman, "In-band full-duplex wireless: challenges and opportunities," *IEEE J. Sel. Areas Commun.* **32**, 1637 (2014).
2. S. K. Sharma, T. E. Bogale, L. B. Le, S. Chatzinotas, X. Wang, and B. Ottersten, "Dynamic spectrum sharing in 5G wireless networks with full-duplex technology: recent advances and research challenges," *IEEE Commun. Surv. Tut.* **20**, 674 (2018).
3. M. Jain, J. I. Choi, T. M. Kim, D. Bharadia, S. Seth, K. Srinivasan, P. Levis, S. Katti, and P. Sinha, "Practical, real-time, full duplex wireless," in *Proceedings of the 17th Annual International Conference on Mobile Computing and Networking* (2011), p. 301.
4. S. Hong, J. Brand, J. Choi, M. Jain, J. Mehlman, S. Katti, and P. Levis, "Applications of self-interference cancellation in 5G and beyond," *IEEE Commun. Mag.* **52**, 114 (2014).
5. K. E. Kolodziej, B. T. Perry, and J. S. Herd, "In-band full-duplex technology: techniques and systems survey," *IEEE Trans. Microwave Theory* **67**, 3025 (2019).

6. E. Everett, A. Sahai, and A. Sabharwal, "Passive self-interference suppression for full-duplex infrastructure nodes," *IEEE Trans. Wireless Commun.* **13**, 680 (2014).
7. B. Debaillie, D. Broeck, C. Lavín, B. Liempd, E. A. M. Klumperink, C. Palacios, J. Craninckx, B. Nauta, and A. Pärssinen, "Analog/RF solutions enabling compact full-duplex radios," *IEEE J. Sel. Areas Commun.* **32**, 1662 (2014).
8. T. Riihonen, S. Werner, and R. Wichman, "Mitigation of loopback self-interference in full-duplex MIMO relays," *IEEE Trans. Signal Process.* **59**, 5983 (2011).
9. D. Korpi, T. Riihonen, V. Syrjälä, L. Anttila, M. Valkama, and R. Wichman, "Full-duplex transceiver system calculations: analysis of ADC and linearity challenges," *IEEE Trans. Wirel. Commun.* **13**, 3821 (2014).
10. J. Capmany and D. Novak, "Microwave photonics combines two worlds," *Nat. Photon.* **1**, 319 (2007).
11. R. W. Ridgway, C. L. Dohrman, and J. A. Conway, "Microwave photonics programs at DARPA," *J. Lightwave Technol.* **32**, 3428 (2014).
12. M. Li and N. H. Zhu, "Recent advances in microwave photonics," *Front. Optoelectron.* **9**, 160 (2016).
13. X. Zou, W. Bai, W. Chen, P. Li, B. Lu, G. Yu, W. Pan, B. Luo, L. Yan, and L. Shao, "Microwave photonics for featured applications in high-speed railways: communications detection and sensing," *J. Lightwave Technol.* **36**, 4337 (2018).
14. K. Xu, R. Wang, Y. Dai, F. Yin, J. Li, Y. Ji, and J. Lin, "Microwave photonics: radio-over-fiber links, systems, and applications," *Photon. Res.* **2**, B54 (2014).
15. P. Ghelfi, F. Laghezza, F. Scotti, G. Serafino, A. Capria, S. Pinna, D. Onori, C. Porzi, M. Scaffardi, A. Malacarne, V. Vercesi, E. Lazzari, F. Berizzi, and A. Bogoni, "A fully photonics-based coherent radar system," *Nature* **507**, 341 (2014).
16. V. J. Urick, M. E. Godinez, and D. C. Mikeska, "Photonic assisted radio-frequency interference mitigation," *J. Lightwave Technol.* **38**, 1268 (2020).
17. S. J. Zhang, S. L. Xiao, Y. H. Zhang, H. L. Feng, L. Zhang, and Z. Zhou, "Directly modulated laser based optical radio frequency self-interference cancellation system," *Opt. Eng.* **55**, 026116 (2016).
18. N. N. Shi, Q. Song, J. Tang, W. Li, N. H. Zhu, and M. Li, "A switchable self-interference cancellation system for dual-band IBFD system using a monolithic integrated DML array," *Opt. Commun.* **447**, 55 (2019).
19. Q. Zhou, H. L. Feng, G. Scott, and M. P. Fok, "Wideband co-site interference cancellation based on hybrid electrical and optical techniques," *Opt. Lett.* **39**, 6537 (2014).
20. Y. Zhang, S. Xiao, Y. Yu, C. Chen, M. Bi, L. Liu, L. Zhang, and W. Hu, "Experimental study of wideband in-band full-duplex communication based on optical self-interference cancellation," *Opt. Express* **24**, 30139 (2016).
21. J. J. Sun, M. P. Chang, and P. R. Prucnal, "Demonstration of over-the-air RF self-interference cancellation using an optical system," *IEEE Photon. Tech. Lett.* **29**, 397 (2017).
22. Y. H. Zhang, L. S. Li, S. L. Xiao, M. H. Bi, Y. H. Yu, and W. S. Hu, "Wideband over-the-air RF self-interference cancellation by an EML-based optical system with baseband predistortion," *IEEE Photon. J.* **9**, 5503009 (2017).
23. Y. H. Zhang, L. S. Li, S. L. Xiao, M. H. Bi, L. Huang, L. Z. Zheng, and W. S. Hu, "EML-based multi-path self-interference cancellation with adaptive frequency-domain pre-equalization," *IEEE Photon. Tech. Lett.* **30**, 1103 (2018).
24. M. P. Chang, M. Fok, A. Hofmaier, and P. R. Prucnal, "Optical analog self-interference cancellation using electro-absorption modulators," *IEEE Microwave Wireless Comp.* **23**, 99 (2013).
25. X. Y. Han, B. F. Huo, Y. C. Shao, C. Wang, and M. S. Zhao, "RF self-interference cancellation using phase modulation and optical sideband filtering," *IEEE Photon. Tech. Lett.* **29**, 917 (2017).
26. X. X. Su, S. L. Fu, S. Wang, X. Yang, P. Y. Wang, C. Wang, Z. L. Wu, Y. Y. Gu, M. S. Zhao, and X. Y. Han, "Performance analysis of photonic RF self-interference cancellation for full-duplex communication," *Proc. SPIE* **11192**, 111920H (2019).
27. F. J. Shi, Y. Y. Fan, X. Y. Wang, Q. G. Tan, and Y. S. Gao, "RF self-interference cancellation for radio-over-fiber link based on dual phase modulation in Sagnac loop," *IEEE Photon. J.* **13**, 7800315 (2021).
28. M. Huang, D. Zhu, and S. Pan, "Optical RF interference cancellation based on a dual-parallel polarization modulator," in *Proceedings of Asia Communications and Photonics Conference* (2014), paper ATh1F.6.
29. W. Zhou, P. Xiang, Z. Niu, M. Wang, and S. Pan, "Wideband optical multipath interference cancellation based on a dispersive element," *IEEE Photon. Tech. Lett.* **28**, 849 (2016).
30. Y. Xiang, G. Li, and S. Pan, "Ultrawideband optical cancellation of RF interference with phase change," *Opt. Express* **25**, 21259 (2017).
31. J. Suarez, K. Kravtsov, and P. R. Prucnal, "Incoherent method of optical interference cancellation for radio-frequency communications," *IEEE J. Quantum Electron.* **45**, 402 (2009).
32. Z. Y. Tu, A. J. Wen, X. R. Li, and H. X. Zhang, "A photonic pre-distortion technique for RF self-interference cancellation," *IEEE Photon. Tech. Lett.* **30**, 1297 (2018).
33. S. Wang, X. Y. Han, B. F. Huo, H. Q. Wang, X. X. Su, Y. C. Shao, Z. L. Wu, and M. S. Zhao, "Optical RF self-interference cancellation using polarization multiplexed dual-MZMs," in *Proceedings of IEEE International Topical Meeting Microwave Photonics* (2018), p. 1.
34. Y. Zhang, S. Xiao, H. Feng, L. Zhang, Z. Zhou, and W. Hu, "Self-interference cancellation using dual-drive Mach-Zehnder modulator for in-band full-duplex radio-over-fiber system," *Opt. Express* **23**, 33205 (2015).
35. X. Y. Han, B. F. Huo, Y. C. Shao, and M. S. Zhao, "Optical RF self-interference cancellation by using an integrated dual-parallel MZM," *IEEE Photon. J.* **9**, 5501308 (2017).
36. X. Han, B. Huo, Y. Shao, S. Wang, and M. Zhao, "RF self-interference cancellation for full-duplex communication with microwave photonic technique," in *Proceedings of IEEE International Topical Meeting Microwave Photonics* (2017), p. 1.
37. X. Li, Y. Zhang, L. Huang, L. Deng, M. Cheng, S. Fu, M. Tang, and D. M. Liu, "Optimized self-interference cancellation based on optical dual-parallel MZM for co-frequency and co-time full duplex wireless communication under nonlinear distortion and emulated multipath effect," *Opt. Express* **27**, 37286 (2019).
38. J. Chang and P. R. Prucnal, "A novel analog photonic method for broadband multipath interference cancellation," *IEEE Microwave Wireless Comp. Lett.* **23**, 377 (2013).
39. F. Shen, X. Su, S. Fu, C. Li, S. Yang, Z. Wu, Y. Gu, Q. Tan, K. Zhu, M. Zhao, and X. Han, "Simulation and performance analysis of photonic integrated RF self-interference cancellation system," *Acta Photon. Sin.* **48**, 1148017 (2019).
40. M. P. Chang, A. Tait, J. Chang, and P. R. Prucnal, "An integrated optical interference cancellation system," in *Wireless and Optical Communication Conference* (2014), paper O5.4.
41. K. E. Kolodziej, S. Yegnanarayanan, and B. T. Perry, "Photonic-enabled RF canceller for wideband in-band full-duplex wireless systems," *IEEE Trans. Microwave Theory* **67**, 2076 (2019).
42. K. E. Kolodziej, S. Yegnanarayanan, and B. T. Perry, "Fiber Bragg grating delay lines for wideband self-interference cancellation," *IEEE Trans. Microwave Theory* **67**, 4005 (2019).
43. M. P. Chang, C.-L. Lee, B. Wu, and P. R. Prucnal, "Adaptive optical self-interference cancellation using a semiconductor optical amplifier," *IEEE Photon. Tech. Lett.* **27**, 1018 (2015).
44. Q. Zhou, J. Ge, and M. Fok, "Fast dynamic in-band RF self-interference cancellation for enabling efficient spectral range," in *Optical Fiber Communications Conference and Exhibition (OFC)* (2017), paper W4B.5.
45. Y. H. Zhang, L. S. Li, M. H. Bi, and S. L. Xiao, "Over-the-air in-band full-duplex system with hybrid RF optical and baseband digital self-interference cancellation," *Opt. Commun.* **405**, 152 (2017).
46. X. Y. Han, X. C. Chen, and J. P. Yao, "Simultaneous even- and third-order distortion suppression in a microwave photonic link based on orthogonal polarization modulation, balanced detection and optical sideband filtering," *Opt. Express* **24**, 14812 (2016).
47. E. C. Blow, M. P. Chang, and P. R. Prucnal, "Microwave photonic interference canceller: noise figure reduction via balanced architecture," in *International Topical Meeting on Microwave Photonics* (2016), p. 157.
48. X. Y. Han, E. M. Xu, W. L. Liu, and J. P. Yao, "Tunable dual-passband microwave photonic filter using orthogonal polarization modulation," *IEEE Photon. Tech. Lett.* **27**, 2209 (2017).
49. M. P. Chang, N. Wang, B. Wu, and P. R. Prucnal, "A simultaneous variable optical weight and delay in a semiconductor optical amplifier for microwave photonics," *J. Lightwave Technol.* **33**, 2120 (2015).
50. W. Xue and J. Mørk, "Tunable true-time delay of a microwave photonic signal realized by cross gain modulation in a semiconductor waveguide," *Appl. Phys. Lett.* **99**, 231102 (2011).
51. T. Huusari, Y. Choi, P. Liikkanen, D. Korpi, S. Talwar, and M. Valkama, "Wideband self-adaptive RF cancellation circuit for full-duplex radio:

- operating principle and measurements," in *2015 IEEE 81st Vehicular Technology Conference (VTC Spring)* (2015), p. 1.
52. K. E. Kolodziej, J. G. McMichael, and B. T. Perry, "Multitap RF canceller for in-band full-duplex wireless communications," *IEEE Trans. Wireless Commun.* **15**, 4321 (2016).
 53. M. P. Fok, Y. Deng, K. Kravtsov, and P. R. Prucnal, "Signal beating elimination using single-mode fiber to multimode fiber coupling," *Opt. Lett.* **36**, 4578 (2011).
 54. D. Chapman, "Low-loss many-to-one fiber couplers with few or single-mode inputs and a multi-mode output," *Fiber Integrated Opt.* **23**, 375 (2004).
 55. H. Zhang, S. Pan, M. Huang, and X. Chen, "Polarization-modulated analog photonic link with compensation of the dispersion-induced power fading," *Opt. Lett.* **37**, 866 (2012).
 56. X. X. Su, X. Y. Han, S. L. Fu, S. Wang, C. Li, Q. G. Tan, G. Zhu, C. Wang, Z. L. Wu, Y. Y. Gu, and M. S. Zhao, "Optical multipath RF self-interference cancellation based on phase modulation for full-duplex communication," *IEEE Photon. J.* **12**, 7102114 (2020).
 57. P. J. Winzer, D. T. Neilson, and A. R. Chraplyvy, "Fiber-optic transmission and networking: the previous 20 and the next 20 years," *Opt. Express* **26**, 24190 (2018).
 58. G. Lazarev, P. Chen, J. Strauss, N. Fontaine, and A. Forbes, "Beyond the display: phase-only liquid crystal on silicon devices and their applications in photonics," *Opt. Express* **27**, 16206 (2019).
 59. R. Waterhouse and D. Novack, "Realizing 5G: microwave photonics for 5G mobile wireless systems," *IEEE Microwave Mag.* **16**, 84 (2015).
 60. S. Pan, D. Zhu, S. F. Liu, K. Xu, Y. T. Dai, T. L. Wang, J. G. Liu, N. H. Zhu, Y. Xue, and N. J. Liu, "Satellite payloads pay off," *IEEE Microwave Mag.* **16**, 61 (2015).
 61. D. Marpaung, J. Yao, and J. Capmany, "Integrated microwave photonics," *Nat. Photon.* **13**, 80 (2019).
 62. M. Smit, X. Leijtens, H. Ambrosius, E. Bente, J. van der Tol, B. Smalbrugge, T. de Vries, E.-J. Geluk, J. Bolk, R. van Veldhoven, L. Augustin, P. Thijs, D. D'Agostino, H. Rabbani, K. Lawniczuk, S. Stopinski, S. Tahvili, A. Corradi, E. Kleijn, D. Dzibrou, M. Felicetti, E. Bitincka, V. Moskalenko, J. Zhao, R. Santos, G. Gilardi, W. Yao, K. Williams, P. Stabile, P. Kuindersma, J. Pello, S. Bhat, Y. Jiao, D. Heiss, G. Roelkens, M. Wale, P. Firth, F. Soares, N. Grote, M. Schell, H. Debregeas, M. Achouche, J.-L. Gentner, A. Bakker, T. Korthorst, D. Gallagher, A. Dabbs, A. Melloni, F. Morichetti, D. Melati, A. Wonfor, R. Penty, R. Broeke, B. Musk, and D. Robbins, "An introduction to InP-based generic integration technology," *Semicond. Sci. Tech.* **29**, 083001 (2014).
 63. J. van der Tol, Y. Jiao, J. van Engelen, V. Pogoretskiy, A. Kashi, and K. Williams, "InP membrane on silicon (IMOS) photonics," *IEEE J. Quantum Electron.* **56**, 6300107 (2020).
 64. M. P. Chang, E. C. Blow, J. J. Sun, M. Z. Lu, and P. R. Prucnal, "Integrated microwave photonic circuit for self-interference cancellation," *IEEE Trans. Microwave Theory* **65**, 4493 (2017).
 65. M. P. Chang, E. C. Blow, M. Z. Lu, J. J. Sun, and P. R. Prucnal, "RF characterization of an integrated microwave photonic circuit for self-interference cancellation," *IEEE Trans. Microwave Theory* **66**, 596 (2018).
 66. L. J. Wang, A. Kuzmich, and A. Dogariu, "Gain-assisted superluminal light propagation," *Nature* **406**, 277 (2000).
 67. M. Piqueras, G. Grosskopf, B. Vidal, J. H. Llorente, J. M. Martinez, P. Sanchis, V. Polo, J. L. Corral, A. Marceaux, J. Galière, J. Lopez, A. Enard, J.-L. Valard, O. Parillaud, E. Estèbe, N. Vodjdani, M.-S. Choi, J. H. den Besten, F. M. Soares, M. K. Smit, and J. Marti, "Optically beamformed beam-switched adaptive antennas for fixed and mobile broad-band wireless access networks," *IEEE Trans. Microwave Theory* **54**, 887 (2006).
 68. B. Jalali and S. Fathpour, "Silicon photonics," *J. Lightwave Technol.* **24**, 4600 (2006).
 69. M. Hochberg and T. Baehr-Jones, "Towards fabless silicon photonics," *Nat. Photon.* **4**, 492 (2010).
 70. A. Rahim, J. Goyvaerts, B. Szelag, J.-M. Fedeli, P. Absil, T. Aalto, M. Harjanne, C. G. Littlejohns, G. T. Reed, G. Winzer, S. Lischke, Z. Lars, D. Knoll, D. Geuzebroek, A. Leinse, M. Geiselmann, M. Zervas, H. Jans, A. Stassen, C. Dominguez, P. Munoz, D. Domenech, A. L. Giesecke, M. C. Lemme, and R. Baets, "Open-access silicon photonics platforms in Europe," *IEEE J. Sel. Top. Quantum Electron.* **25**, 8200818 (2019).
 71. X. Han, "Research advances in microwave photonic active cancellation technology," in *5th Microwave Photonics Technology and Application Symposium* (2020), p. 1.
 72. M. Tang, J. Park, Z. Wang, S. Chen, P. Jurczak, A. Seeds, and H. Liu, "Integration of III-V lasers on Si for Si photonics," *Prog. Quant. Electron.* **66**, 1 (2019).
 73. L. Zheng, S. Xiao, Z. Liu, M. P. Fok, J. Fang, H. Yang, M. Lu, Z. Zhang, and W. Hu, "Adaptive over-the-air RF self-interference cancellation using a signal-of-interest driven regular triangle algorithm," *Opt. Lett.* **45**, 1264 (2020).
 74. L. Zheng, Z. Liu, S. Xiao, M. P. Fok, Z. Zhang, and W. Hu, "Hybrid wideband multipath self-interference cancellation with an LMS pre-adaptive filter for in-band full-duplex OFDM signal transmission," *Opt. Lett.* **45**, 6382 (2020).
 75. L. Huang, Y. Zhang, S. Xiao, L. Zheng, and W. Hu, "Real-time adaptive optical self-interference cancellation system for in-band full-duplex transmission," *Opt. Commun.* **437**, 259 (2019).
 76. L. Zheng, Y. Zhang, S. Xiao, L. Huang, J. Fang, and W. Hu, "Adaptive optical self-interference cancellation for in-band full-duplex systems using regular triangle algorithm," *Opt. Express* **27**, 4116 (2019).
 77. H. Wang, "Research on microwave photonics RF interference cancellation feedback control technology," Ph.D Thesis (Dalian University of Technology, 2019).
 78. W. Bai, X. Zou, P. Li, W. Pan, L. Yan, B. Luo, and X. Lu, "A WDM-PON compatible wavelength-reused bidirectional in-band full-duplex radio-over-fiber system," *Opt. Commun.* **463**, 125408 (2020).
 79. Y. Chen and J. Yao, "Photonic-assisted RF self-interference cancellation with improved spectrum efficiency and fiber transmission capability," *J. Lightwave Technol.* **38**, 761 (2020).
 80. Y. Chen, "A photonic-based wideband RF self-interference cancellation approach with fiber dispersion immunity," *J. Lightwave Technol.* **38**, 4618 (2020).
 81. Y. Chen and S. Pan, "Simultaneous wideband radio-frequency self-interference cancellation and frequency downconversion for in-band full-duplex RoF systems," *Opt. Lett.* **43**, 3124 (2018).
 82. S. Zhu, M. Li, N. Zhu, and W. Li, "Photonic radio frequency self-interference cancellation and harmonic down-conversion for in-band full-duplex radio-over-fiber system," *IEEE Photon. J.* **11**, 5503110 (2019).
 83. D. Zhu, X. Hu, W. Chen, D. Ben, and S. Pan, "Photonics-enabled simultaneous self-interference cancellation and image-reject mixing," *Opt. Lett.* **44**, 5541 (2019).
 84. B. Weng, Y. Chen, and Y. Chen, "Photonic-assisted wideband frequency downconverter with self-interference cancellation and image rejection," *Appl. Opt.* **58**, 3539 (2019).
 85. L. Huang, Y. Zhang, X. Li, L. Deng, M. Chen, S. Fu, M. Tang, and D. Liu, "Microwave photonic RF front-end for co-frequency co-time full duplex 5G communication with integrated RF signal self-interference cancellation, optoelectronic oscillator and frequency down-conversion," *Opt. Express* **27**, 32147 (2019).
 86. J. Wang, Y. Wang, Z. Zhang, Z. Zhao, and J. Liu, "Optical self-interference cancellation with frequency down-conversion based on cascade modulator," *IEEE Photon. J.* **12**, 5502708 (2020).